

## Evidence for a photocurrent Fano resonance in an artificial nanostructure

Tiziana dell'Orto, M. Di Ventra, J. Almeida, C. Coluzza, and G. Margaritondo

*Institute de Physique Appliquée, Ecole Polytechnique Fédérale, PH-Ecublens, CH-1015 Lausanne, Switzerland*

(Received 5 May 1995)

We present internal-photoemission (photocurrent) experimental evidence for a Fano resonance at an  $n$ - $p$  GaAs homojunction with a 0.5-ML Si intralayer ( $\delta$  doping). This is one of a very few cases in which Fano resonances have been observed in artificial nanostructures. Our results show that this fundamental class of phenomena plays a relevant role in band-gap engineering, by affecting the transport and phototransport properties of  $\delta$ -doping nanostructures.

Fano resonances are a fundamental class of phenomena in molecular and solid-state physics.<sup>1,2</sup> They are observed whenever an electromagnetic excitation involves discrete electronic states interacting with one or more continua. Characteristic Fano spectroscopic line shapes have been observed in a large variety of atomic, molecular, and solid-state systems.<sup>3-5</sup> Many theorists did predict Fano resonances in artificial systems, and emphasized their potential technological applications. We note, in particular, that Maschke, Thomas, and Göbel<sup>6</sup> in 1991 predicted Fano resonances in quantum-well structures and, in agreement with Harris,<sup>7</sup> emphasized their importance in phenomena such as "lasing without inversion."<sup>8</sup>

Only recently, however, have phenomena of this type been observed in artificial structures, specifically quantum wells.<sup>4,5</sup> We present evidence for a Fano resonance in a different class of artificial nanostructures, homojunctions with  $\delta$ -doping-induced band discontinuities. Our results indicate that phenomena of this type cannot be ignored when modeling the behavior of band-gap engineering nanostructures,<sup>9</sup> since they significantly affect the transport, phototransport, and optical properties.

We used a thin (0.5 ML) Si intralayer in a GaAs homojunction to create an artificial dipole that changes the alignment in energy of the two band structures of the two sides of the junction. This results in a valence- (and conduction-) band discontinuity of  $0.37 \pm 0.04$  eV.<sup>10-12</sup> The potential profile of the Si-modified structure is schematized as a triangular well (see Fig. 1).

The low-temperature internal photoemission spectra of this structure exhibit two peaks. One is attributed to a resonant state produced by the potential triangular shape [state *A* in Fig. 1(b)]. The second is interpreted as a Fano resonance produced by a localized state,  $\approx 0.34$  eV below the  $n$ -type GaAs conduction-band edge [state *B* in Fig. 1(b)], which couples with the continuum. The presence of state *A* is evidence for the Si intralayer-induced band discontinuity in the GaAs homojunction. Experimental tests supported by a theoretical analysis of the triangular well show that state *B* is *not* a resonant state of the potential well but is instead located in the junction's  $n$ -side gap.

We explain the Fano resonance by assuming for state *B* a localized character, and taking into account its interaction with the conduction-band continuum. On these assumptions,

we were able to theoretically reproduce the characteristic Fano line shape of the spectral feature caused by state *B*.

The nanostructures were grown by molecular-beam epitaxy on  $p^+$ -type GaAs(100) substrates covered by  $1 \mu\text{m}$  of  $p = 1 \times 10^{17} \text{ cm}^{-3}$  GaAs (grown at  $580^\circ\text{C}$ ). 0.5 ML of Si (1 ML =  $6.25 \times 10^{14} \text{ cm}^{-2}$ ) was deposited at  $T = 500^\circ\text{C}$ , followed by  $9 \text{ \AA}$  of GaAs grown at  $250^\circ\text{C}$ , to reduce Si diffusion in the subsequent  $n$  overlayer. The  $n$  overlayer (0.5  $\mu\text{m}$ ,  $n = 1 \times 10^{17} \text{ cm}^{-3}$ ), was grown at  $580^\circ\text{C}$ ; a final  $n$ -doped GaAs layer ( $110 \text{ \AA}$ ,  $n = 5 \times 10^{18} \text{ cm}^{-3}$ ) was added to facilitate the Ohmic contact formation. The maximum uncertainty in the GaAs-layer thicknesses was 20%, therefore irrelevant to our conclusions; the Si-layer thickness was even more accurate.

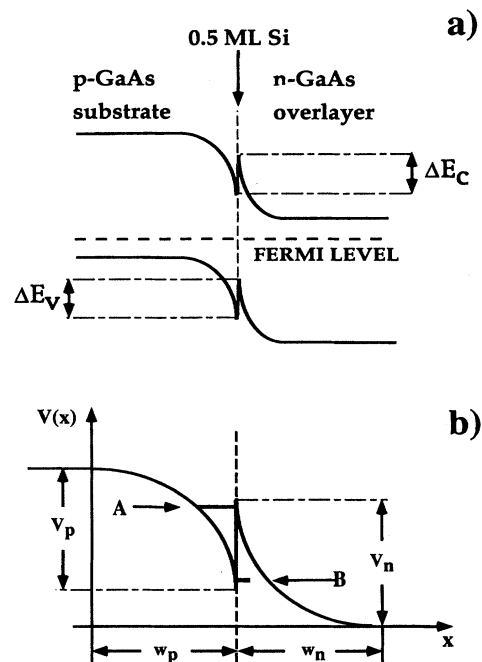


FIG. 1. Band diagram of our  $n$ -type GaAs/0.5-ML Si/ $p$ -type GaAs nanostructure. (a) The Si intralayer creates artificial discontinuities  $\Delta E_c$  and  $\Delta E_v$  in the conduction and valence bands. (b) Enlarged view of the interface, with the two resonant states *A* and *B*. The depletion lengths  $w_n, w_p$  and the potential drops  $V_n, V_p$  are also shown.

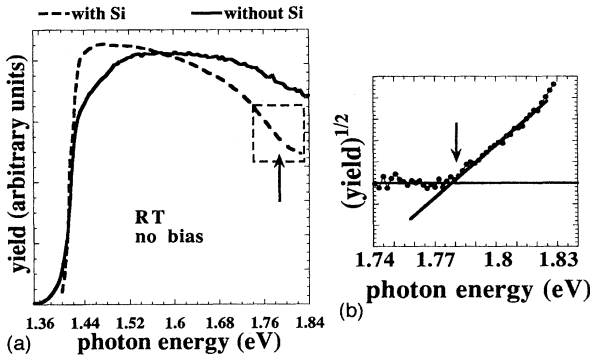


FIG. 2. (a) Photocurrent vs photon-energy spectra at room temperature for *n*-type GaAs/*p*-type GaAs homojunctions with and without a Si intralayer. (b) Square-root plot of the background-subtracted spectrum in the region of the second threshold.

Internal photoemission spectra were taken by illuminating the sample from the overlayer side with monochromatic light and measuring the photocurrent across the junction as a function of the photon energy,<sup>10,13</sup> in the range 1.35–2.2 eV. The photon source was a tungsten lamp coupled to a double-grating monochromator. A chopper modulated the light, and the correspondingly modulated photocurrent was detected with a lock-in amplifier (a beam splitter and a PbS photodiode detector provided the reference signal). Spectra were taken at room temperature and at liquid-nitrogen temperature. For reference, internal photoemission spectra were taken not only on the structures with Si intralayers but also on equivalent structures without intralayers.

Figure 2(a) shows the room-temperature spectra of a reference nanostructure without intralayers and of a Si-intralayer-modified structure. The first threshold at  $\approx 1.41$  eV is due to optical transitions from the top of the valence band to the bottom of the conduction band and corresponds to GaAs gap width. We obtained  $1.41 \pm 0.2$  eV for both structures, in agreement with the literature GaAs gap width.

The second threshold at  $\approx 1.78$  eV, emphasized by the plot of Fig. 2(b), is present only in the spectrum of the Si-modified system. It is due to the excitation from the *p*-side valence-band edge to the *n*-side conduction-band edge, across the artificial band discontinuity created by the Si intralayer. The difference between the two threshold energy positions corresponds to the conduction-band discontinuity  $\Delta E_c$ , which also equals the valence-band discontinuity  $\Delta E_v$ .

The plot of Fig. 2(b) is the square root of the photocurrent after background subtraction, following Fowler's theory.<sup>14</sup> From this plot we derive a threshold position of  $1.78 \pm 0.02$  eV. The threshold position does not change, within the experimental uncertainty, when taking spectra under forward and reverse bias.

From the experimental threshold positions, we estimate that the Si intralayer induces a band discontinuity  $\Delta E_c = 0.37 \pm 0.04$  eV. These results are consistent with our previous internal-photoemission results on the *p*-type GaAs(100) overlayers over *n*-type GaAs(100) substrates<sup>10</sup> and with the conventional photoemission data of Ref. 11. The creation of the discontinuity is theoretically justified by the models of Ref. 15.

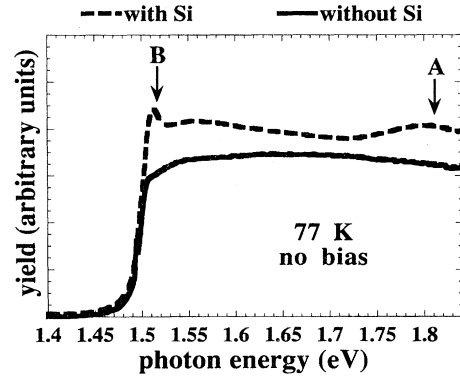


FIG. 3. 77-K spectra corresponding to those of Fig. 2(a). The two arrows indicate peaks A and B, corresponding in our interpretation to states A and B in Fig. 1(b).

The Fig. 3 spectra, taken at liquid-nitrogen temperature, reveal additional spectral features not visible at room temperature, peaks A and B. These features are only visible for the Si-intralayer specimen, and peak A makes it impossible to detect the weak second threshold of Fig. 2(b). The first threshold corresponds to the GaAs gap width at 77 K,  $1.49 \pm 0.02$  eV.

One important point in the identification of the nature of the two peaks is their different dependence on the external bias—see Fig. 4, where a positive bias is a forward bias. The position of peak A changes with the bias, as shown in Fig. 4 for the sample under 0-, -1-, and +1-V bias; furthermore, peak A tends to disappear as we approach the flat-band condition (bias  $\approx 1.4$  V). On the contrary, no change in the position of peak B is detected as the bias changes.

Two different interpretations are thus necessary for the two peaks. As to peak A, an electron excited from the *p*-side valence band to a state inside the triangular conduction well can recombine or scatter through the potential barrier. If the excitation energy is equal to a resonance energy, then the probability of tunneling into the *n* side is maximized, and this produces a maximum in the photocurrent—peak A.

We theoretically estimated the position of peak A by finding resonances of the triangular potential of Fig. 1, neglecting any inelastic processes. We calculated the phase shift of

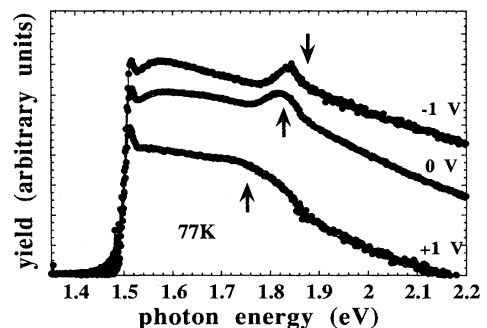


FIG. 4. 77-K spectra for the *n*-type GaAs/*p*-type GaAs homojunctions with a Si intralayer under different biases. The arrows indicate the theoretically calculated positions of peak A.

the reflection amplitude with a variable-phase-like method.<sup>16</sup> The energy position of the resonances are the peaks of the derivative of the phase shift with respect to the particle momentum. Details of the method will be given in a forthcoming paper.<sup>17</sup> The method is exact, in the sense that the only approximation is the form of the potential well, which was assumed to be

$$V(x) = \begin{cases} V_p + V_n - \Delta E_c - (V_p/w_p)x^2 & \text{for } 0 \leq x < w_p \\ (V_n/w_n)(x - w_n - w_p)^2 & \text{for } w_p \leq x \leq w_n, \end{cases}$$

where  $V_p$  and  $V_n$  are the potential drops without Si, plus one-half of the onset produced by the Si on the  $p$  and  $n$  sides [Fig. 1(b)]. The depletion lengths  $w_n$  and  $w_p$  were calculated assuming that the Si intralayer atoms are distributed in an acceptor and donor bilayer, and, due to the high concentration of Si, evaluated as  $w_n = (2\epsilon V_n/en)^{1/2}$  and  $w_p = (2\epsilon V_p/ep)^{1/2}$  (Ref. 18), where  $e$  is the electronic charge and  $\epsilon$  is the dielectric constant.

At zero bias, we calculated  $V_p = V_n = 0.89$  eV,  $w_p = w_n = 87$  Å and assuming  $0.067m_e$  for the GaAs electron mass we obtained a first resonant state at 1.83 eV. After adding the external bias, this resonance shifts to 1.75 eV for +1-V bias and to 1.88 eV for -1-V bias. The arrows in Fig. 4 show that these theoretical positions qualitatively reproduce the experimental peak shifts with the bias. Note that the presence of peak A and its bias dependence is directly related to the Si-induced band discontinuity that creates the triangular well. The reasonable agreement between theory and experiment corroborates our choice for the potential shape.

Our theoretical explanation of peak A and of its bias dependence implies that peak B has a different origin. The line shape, with its characteristic high-energy antiresonance, immediately suggests a Fano-resonance mechanism. A Fano resonance can indeed be explained by the coupling of a discrete localized state [state B in Fig. 1(b)] with the continuum of states in the conduction band.

We best-fitted peak B with a Fano-resonance line shape  $A(\xi - q)^2 / (1 + \xi^2)$ , where  $A$  is a constant, and  $q$  is the ratio between the optical matrix elements of the transitions to the discrete state and the continuum;  $\xi = (E_0 - E)/\Gamma$ , where  $E$  is the photon energy,  $E_0$  is the energy position of the discrete state, and  $\Gamma$  is the strength of the coupling between the discrete state and the continuum.<sup>1,2</sup> We assumed zero  $k$  dispersion in the interface plane.<sup>6</sup> Figure 5 shows the results of the

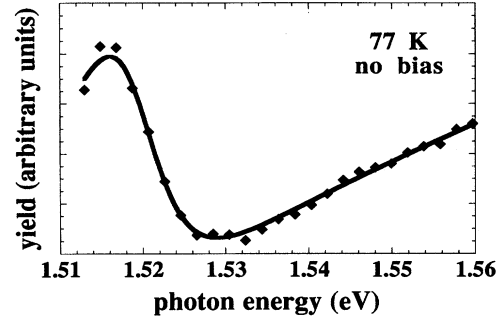


FIG. 5. Fano-line-shape fit of the 77-K no-bias spectrum of Fig. 4.

least-square best fit, obtained for  $q = -1.9$ ,  $\Gamma = 7 \times 10^{-3}$  eV, and  $E_0 = 1.520$  eV at zero bias.

After fitting the data for +1- and -1-V bias, we found that the estimated position of state B,  $E_0 = 1.520$  eV, remained unchanged within 2 meV, explaining the experimental peak-B position insensitivity to the bias.

Therefore, this insensitivity supports the interpretation based on a Fano resonance, related to a discrete state  $A \approx 0.34$  eV below the bottom of the  $n$ -side conduction band and not related to the potential shape. The nature of this state is not identified, and only speculatively can we propose that it is a Si-induced state in the  $n$ -side GaAs gap.

This uncertainty, however, does not affect the twofold importance of our results: First, they provide evidence for a Fano resonance in nanostructures based on  $\delta$ -doping-induced band discontinuities, in the spirit of band-gap engineering. Furthermore, resonant states like those we derived from our spectra can play a fundamental role in band-gap engineering by affecting the transport, phototransport, and other properties of nanostructures.

We are grateful to L. Sorba, M. Lazzarino, and A. Franciosi for their help in the development of the nanostructures used in these experiments. We are also indebted to M. Sassoli de Bianchi, N. Binggeli, K. Maschke, and A. Baldereschi for many useful discussions. This work was supported by the Swiss National Project "Sciences, Applications et Technologies Optiques," by the Swiss National Science Foundation, and by the Ecole Polytechnique Fédérale de Lausanne.

<sup>1</sup>U. Fano, Phys. Rev. **124**, 1866 (1961).

<sup>2</sup>U. Siegner, M.-A. Mweck, S. Glutsch, and D. S. Chemla, Phys. Rev. Lett. **74**, 470 (1995).

<sup>3</sup>*Electron and Photon Interaction with Atoms*, edited by H. Klei-poppen and M. R. C. McDowell (Plenum, New York, 1976); J. J. Hopfield, P. J. Dean, and D. J. Thomas, Phys. Rev. **158**, 748 (1967).

<sup>4</sup>L. A. O. Nunes, L. Ioratti, L. T. Flores, and J. P. Harbison Phys. Rev. B **47**, 13 011 (1993), and references therein; Kui-juan Jin, Shao-hua Pan, and Guo-zhen Yang, *ibid.* **50**, 8584 (1994), and references therein.

<sup>5</sup>D. Y. Oberli, G. Böhm, G. Weimann, and J. A. Brum, Phys. Rev. B **49**, 5757 (1994).

<sup>6</sup>K. Maschke, P. Thomas, and E. O. Göbel, Phys. Rev. Lett. **67**, 2646 (1991).

<sup>7</sup>S. E. Harris, Phys. Rev. Lett. **62**, 1033 (1989).

<sup>8</sup>V. G. Arkhipkin and Yu. I. Heller, Phys. Lett. **98A**, 12 (1983).

<sup>9</sup>F. Capasso, K. Mohammed, and A. Y. Cho, J. Vac. Sci. Technol. B **3**, 1245 (1985).

<sup>10</sup>Tiziana dell'Orto, J. Almeida, C. Coluzza, A. Baldereschi, G. Margaritondo, M. Cantile, S. Yildirim, L. Sorba, and A. Franciosi, Appl. Phys. Lett. **64**, 2111 (1994).

- <sup>11</sup>M. Marsi, R. Houdré, A. Rudra, M. Ilegems, F. Gozzo, C. Coluzza, and G. Margaritondo, *Phys. Rev. B* **47**, 6455 (1993).
- <sup>12</sup>Tiziana dell'Orto, Gelsomina De Stasio, M. Capozzi, C. Ottaviani, C. Quaresima, and P. Perfetti, *Phys. Rev. B* **48**, 8823 (1993).
- <sup>13</sup>G. Abstreiter, U. Prechtel, G. Weimann, and W. Schlapp, *Physica* **134B**, 433 (1985).
- <sup>14</sup>R. H. Fowler, *Phys. Rev.* **38**, 45 (1931).
- <sup>15</sup>W. A. Harrison, E. A. Kraut, J. R. Waldrop, and R. W. Grant, *Phys. Rev. B* **18**, 4402 (1978); W. A. Harrison, *J. Vac. Sci. Technol.* **16**, 1492 (1979); A. Muñoz, N. Chetty, and R. M. Martin, *Phys. Rev. B* **41**, 2976 (1990); K. Kunc and R. M. Martin, *ibid.* **24**, 3445 (1981); R. G. Dandrea, S. Froyen, and A. Zunger, *ibid.* **42**, 3213 (1990); M. Peressi, S. Baroni, R. Resta, and A. Baldereschi, *ibid.* **43**, 7347 (1991).
- <sup>16</sup>M. G. Rozman, P. Reineker, and R. Tehver, *Phys. Rev. A* **49**, 3310 (1994); M. Sassoli de Bianchi and M. Di Ventra, *Eur. J. Phys.* (to be published).
- <sup>17</sup>M. Di Ventra and Tiziana dell'Orto (unpublished).
- <sup>18</sup>S. M. Sze, *Physics of Semiconductor Devices* (Wiley, New York, 1981).